Analysis of Radon Near-Surface Measurements, Using Co-Located Ozone Data, Radio-Sounding Vertical Profiles, Sensible Heat Flux and Back-Trajectory Calculation

Giovanni Pitari,[1] Gabriele Curci,[1,2] Vincenzo Rizi,[1,2] Marco Iarlori,[1,2] and Paolo Tuccella[1,2]

Abstract—Simultaneous and co-located observations of near-surface Radon-222, ozone and meteorological parameters in a central Italy observation site operated by the University of L'Aquila (Italy), are used to study the physical drivers of the radon abundance during night-time hours. The knowledge of the potential temperature vertical gradient in the surface layer of nocturnal thermal inversion is made possible using co-located radio-sounding vertical profiles of pressure and temperature, thus making possible to indirectly infer the local surface flux of atmospheric radon (16 ± 6 mBq m^{-2} s^{-1}). The dynamical removal due to turbulent convective motions is found to be the dominant controlling process, determining large differences in the near-surface radon abundance between stable and unstable conditions of the nocturnal Planetary Boundary Layer (PBL). Usual unstable PBL conditions during daytime hours induce an effective dynamical vertical dilution of surface radon, which rapidly reaches a quasi-steady-state abundance during mid-day and afternoon hours, with very low concentration values (5.1 ± 2.0 Bq m^{-3}). Using back-trajectory reanalyses, estimates of local radon fluxes and vertical mixing efficiencies inside the PBL along the air mass latitudinal-longitudinal path and finally the irreversible radon loss due to radioactive decay, we have explored the fraction of daytime radon attributable to long-range advection in the continental near-mountain measurement site of L'Aquila ($44 \pm 18\%$).

Keywords: Atmospheric radio-sounding, Back-trajectory analysis, Near-surface radon, Planetary boundary layer, Sensible heat flux.

[1] Department of Physical and Chemical Sciences, University of L'Aquila, 67100 L'Aquila, Italy. E-mail: paolo.tuccella@univaq.it

[2] Center of Excellence in Telesensing of Environment and Model Prediction of Severe Events (CETEMPS), University of L'Aquila, 67100 L'Aquila, Italy.

1. Introduction

Radon (Rn-222) is a radioactive noble gas emitted from soils into the atmosphere, with a time constant for radioactive decay of approximately 5.5 days. Radon originates from the decay chain of Uranium-238 and produces a solid radioactive progeny (mainly Po-218 and Po-214), that may attach to atmospheric aerosol particles. Vertical and horizontal transport of aerosol particles in the atmospheric boundary layer may then efficiently spread out these alpha particle emitters away from the radon source. A review of the potential health effects of radon is presented in Al-Zoughool and Krewski (2009).

The surface emission flux is on average close to 1 Rn-atoms cm^{-2} s^{-1} over continental sites and close to zero over the oceans or snow/ice covered surfaces (Zahorowski et al., 2013). Several studies produced a local estimation of radon flux as a function of soil water saturation and temperature (Albert et al., 2021; Grossi et al., 2011; Hirao et al., 2010; Perrino et al., 2001). On a global scale, the radioactive decay represents the main sink for atmospheric radon, whereas the space–time local variability is governed by coupling of soil emissions and vertical mixing due to small-scale convective motions in the planetary boundary layer (PBL). For these reasons, radon may be considered a natural tracer of motions in the PBL (Williams et al., 2013). It is more uncertain to what extent the soil moisture can affect radon emissions (Galmarini, 2006), as well as on-going seismic activity (Cicerone et al., 2009).

The vertical transport of atmospheric tracers above the surface is highly correlated with the conditions of dynamical instability of the boundary layer (Crawford et al., 2015; Liu et al., 1984). During

daylight hours the Earth surface warms up through absorption of the incoming solar radiation and becomes convectively unstable. Air masses in the PBL are efficiently mixed up, thus diluting natural tracers (as biogenic volatile organic compounds (BVOC), radon, primary aerosols) or anthropogenic pollutants (as NOx, CO, volatile organic compounds (VOC), particulate matter (PM)) in a thick layer of approximately 1.0–1.5 km above the surface. At night, on the other hand, the boundary layer atmosphere is highly stratified and dynamically stable, thus favouring accumulation of natural tracers and anthropogenic pollutants in a very thin layer above the surface (few tenths of meters), where a strong temperature inversion is present (typically $dT/dz > 2$ K hm^{-1}). In some cases, the night time tracer accumulation is balanced (or overbalanced) by a rapid surface dry deposition, as in the case of NOx and aerosols (Pitari et al., 2014). The dry deposition sink is absent for radon and its radioactive decay is rather slow compared to the PBL growth rate of concentration). For these reasons the atmospheric radon tends to accumulate in the nocturnal PBL, reaching the maximum concentration immediately before sunrise. This is not true, however, during meteorologically unstable nights, when the temperature inversion above the surface is not allowed by synoptic scale conditions of dynamical instability (Di Carlo et al., 2007).

Related to this, the study of turbulence and stability in the boundary layer are at the centre of interest. Cassiani et al. (2015) studied the density of particle dispersion in the convective boundary layer. Chambers et al. (2015) studied the characteristics of the surface layer in relation with the radon profiles. Williams et al. (2013) analysed the radon profile in the contest of diurnal temperature cycle and under different meteorological synoptic conditions, in order to classify the stratification of the boundary layer.

As a consequence of the dynamical processes described above, the boundary layer radon concentration presents a typical diurnal cycle with an approximately constant growth rate from evening hours until sunrise (except during meteorologically unstable nights), a fast decrease during early morning hours (due to fast vertical convective mixing and dynamical dilution of the tracer in a much thicker and

unstable PBL during sunlight hours) and finally a rather steady minimum during midday and afternoon hours (Pitari et al., 2015a). In the latter case, the radon soil flux is roughly compensated by its out-flux at the PBL top. An indirect evidence of these physical processes is the clear anti-correlation of near-surface radon with near-surface ozone and wind velocity (Table 1). As discussed in Di Carlo et al. (2007), in sites with limited photochemical production, the PBL ozone concentration is modulated by coupling of vertical mixing and surface dry deposition. The main ozone reservoir, however, is located above the PBL, whereas radon comes from soils. This may explain the anti-correlation in the L'Aquila site, where PBL ozone photochemistry is of secondary importance, except sporadically during summer months.

Another important difference of observed near-surface radon concentration values between night-time and daytime hours, is that in the first case almost all the measured radon abundance is of local origin, with accumulation following soil emission and containment in the very thin PBL layer of thermal inversion. During daytime hours, once the peak nocturnal values have been dynamically diluted in the diurnal unstable and thick PBL, the rather steady values during midday and afternoon hours may result from both local soil emission and fetch effects from remote sites. Taking into account that the e-folding time constant for radioactive decay of radon is approximately 5.5 days, the effects of large-scale transport during afternoon hours may be significant, especially with Southerly winds. In this case, in fact, moving air masses can bring significant amounts of radon, being originated over the Sahara, where the radon atmospheric influx is at least three times larger

Table 1

Correlation coefficients of hourly data of near-surface radon, wind velocity and ozone; seasonal averages over measurements collected in L'Aquila during 2004–2005-2006

	Rn-wind	Rn-O$_3$
Winter (D–J–F)	− 0.45	− 0.66
Spring (M–A–M)	− 0.47	− 0.66
Summer (J–J–A)	− 0.57	− 0.58
Autumn (S–O–N)	− 0.45	− 0.64

with respect to mid-latitude continental sites (IAEA-WMO, 2011). At night, when wind speeds are often low and mixing depths shallow, the observed radon concentrations are primarily related to the local radon flux. Several studies tried to estimate the flux of radon arrived in a specific location and the results have shown the dependence on both soil and atmospheric conditions and that the radon concentration also depends on the seasonal conditions of air masses transport (Berezina et al., 2013; Chambers et al., 2017).

South-west–north-east transport is often important for the Mediterranean region and Southern Europe in general, because it may produce significant perturbations of in-situ originated natural atmospheric tracers, as for example coarse mode aerosols (Pitari et al., 2015b). A rather frequent dynamical process responsible for the dust uplift from western Sahara has been studied in Grams et al. (2010). It is a complex mesoscale feature, which they call the Atlantic Inflow: it starts with sea breeze and the associated front. These are responsible for the dust uplift, which is then followed by large-scale horizontal transport, taking place in the free troposphere toward the Mediterranean region and Central Europe. An Atlantic low-pressure trough extending far south to the western coast of Morocco from the British Islands, coupled to a high-pressure ridge over Northern Africa and the Mediterranean represents the most favorable meteorological condition for efficient transport toward Europe of natural tracers that are abundant in their desert origin sites, including radon.

In past years, one of the goals in the scientific community was to model flux, profile and transport of radon from remote sites. As already discussed, the radon behavior in atmosphere is strictly related to boundary layer processes. Anisimov et al. (2017) used a Lagrangian model of turbulent transport to determine the vertical profiles of radon, his activity and the thermal stratification of the boundary layer. Vinuesa et al. (2007) in their study used a Large Eddy Simulation (LES) to quantify the evolution of radon in the boundary layer and the processes driving the radon behavior in atmosphere. In the present study we present an estimate of the radon flux produced in situ and subsequently a transport simulation from remote sites to quantify the concentration of transported radon that is added to the one produced in situ.

2. Experimental Section

2.1. Near-Surface Radon and Ozone Measurements

Near-surface observations considered for the present study, *i.e.,* radon, ozone and meteorological parameters, have been collected outdoors on the flat roof of the University of L'Aquila building (20 m above the ground surface), approximately 4 km north-west of downtown L'Aquila, in central Italy (42° 22' N, 13° 21' E), from 2004 to2006, and later more sporadically during 2009, 2014 and 2015. The site is located in the Aterno River valley at 680 m above sea level (a.s.l.), between the Gran Sasso and Sirente-Velino mountain chains. This is a typical continental-climate site, far away from strong anthropogenic pollution sources and characterised by cold winters (mean temperature = 3 °C); the hottest month is July, with a mean temperature of 22 °C. Meteorological parameters (i.e., rainfall, wind speed/direction, temperature, relative humidity, incoming solar radiation) are measured with a time resolution of 5 s, as well as ozone mixing ratios using a UV-absorption analyser. Hourly averaged data are finally calculated for all of these quantities. Radon activity concentration is measured with a Silena model 5S instrument using a scintillation Lucas cell technique, with counts integrated over 1 h time intervals to get hourly values of the radon activity concentration (Pitari et al., 2015a). The detection limit of the instrument is 1 Bq m^{-3} and the calibration is performed on-site by the manufacturer using a certified Radium-226 source; the analyser has a typical count efficiency of 18.6 cpm Bq^{-1} and a background of 0.7 cpm measured with pure nitrogen.

We operated a 3-point running mean to smooth some of point-to-point variability in the dataset. We calculated the nocturnal radon accumulation between 0700 pm and 0500 am LT minus the 0700 pm value, for winter and autumn months and between 0800 pm to 0600 am LT minus 0800 pm value for summer and spring months (Chambers et al., 2015; Williams et al., 2016).

This technique is called mean radon pseudo-gradient and through the individuation of the nocturnal stability window we are capable to calculate quartile ranges of the cumulative frequency of radon and the goal of this technique is to obtain a classification in stability class for all the moths present in the dataset (Chambers et al., 2015). In Online Resource 1, we present the quartile range values for the month of March 2004 and a statistical analysis of the 2004–2006 radon data in the L'Aquila site, for calculating the nocturnal radon gradient fraction in stable PBL conditions, on a monthly basis. The clear maximum in June-October (fraction larger than 90% for stable PBL conditions) results from typical meteorological conditions the Mediterranean area, normally dominated by high pressure conditions and rather dry soils. This maximizes radon release from the ground and minimizes vertical mixing with the free troposphere. Winter-spring months, on the other hand, are more often interested by low pressure disturbances, thus producing more frequent unstable conditions for the nocturnal PBL, as well as more frequent episodes of rainfall or snowfall. During these months, the calculated fraction of stable PBL conditions ranges between 30 and 70%, again using the nocturnal radon gradient as a proxy for estimating the PBL stability conditions.

Starting from the stability categories, we selected the 20% of the most stable night for each month and we compared wind speed values, radon and ozone concentrations with respect to the values of the 20% of well mixed night for the same variable. During stable nights there are low wind speed values between 0 and 1 m/s with a single daytime peak of 2.5 m/s, while unstable nights have values above 2.5 m/s for most of the profile. This directly reflects on the concentrations of Radon and Ozone which present their typical daily cycle of accumulation and mixing (or depletion in the case of ozone). In unstable nights the profile is not very clear, producing a general flattening of the daily cycle for both radon and ozone.

The dynamical driver of the night-time near-surface radon accumulation is clear from Fig. 1. Peaks of 20–40 Bq m^{-3} take place only when the dynamical dilution in the nocturnal PBL is limited by conditions of pronounced atmospheric stability, with very low wind speeds (< 0.7 m s^{-1}) and with rather
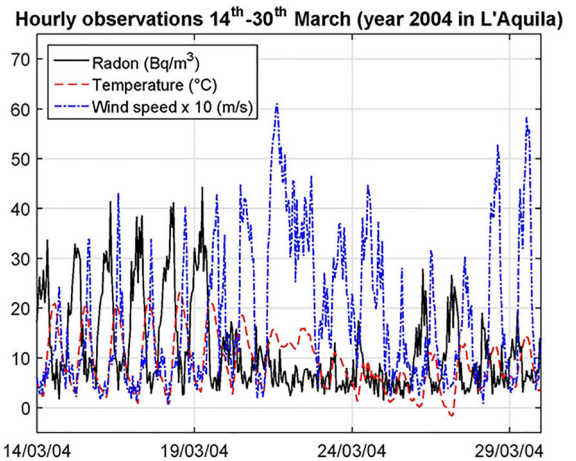

Figure 1
Hourly observations of near-surface atmospheric radon activity concentration (Bq m^{-3}), temperature (K) and wind speed (dm s^{-1}), in the time period 14–30 March 2004, at L'Aquila (Italy)

fast nocturnal temperature cooling rates (> 0.5 K h^{-1}). In the March 2004 time-series presented in Fig. 1, these two conditions are not simultaneously met in the period 20–25 March, making a clear radon nocturnal increase not possible.

As previously discussed in the introduction, the pronounced correlation of the nocturnal radon accumulation with the simultaneous near-surface ozone
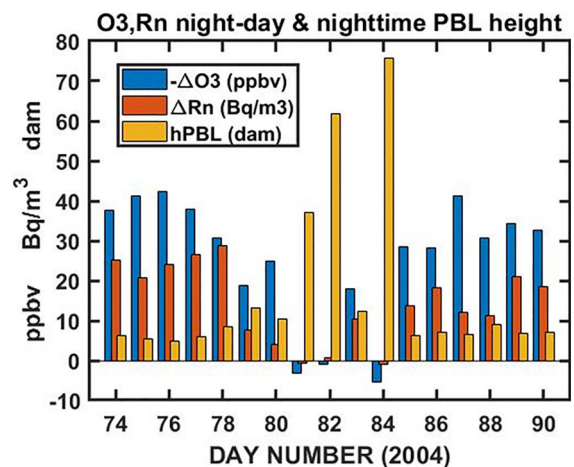

Figure 2
Differences between night and day average values of near-surface ozone mixing ratio (ppbv, blue bars) and radon activity concentration (Bq m^{-3}, red bars), superimposed to the night-time PBL height (decameters, yellow bars), for the same time period shown in Fig. 1. The PBL height is obtained following the procedure described in the text (Eq. 1–4)

decrease under conditions of a stable PBL (Fig. 2) is another clear evidence of the dynamical driver of atmospheric radon (Pitari et al., 2015a).

Table 1 summarizes the hourly data correlation coefficients of radon-wind and radon-ozone. The lower Rn-O$_3$ correlation during summer months is consequence of a more active ozone photochemistry in the PBL during daytime hours the PBL during daytime hours (Di Carlo et al., 2007).

2.2. Atmospheric Radio-Sounding

Since 1994, DSFC/CETEMPS at the of University of L'Aquila has operated a ptu (pressure, temperature, relative humidity) and ozone-sonde station (42.38N, 13.31E, site elevation 683 m a.s.l.). In the period 2000–2016 the quality-checked balloon-borne ozone measurements conducted in troposphere and stratosphere were 295; ptu measurements were 450 in total. In some periods the observational activity was stopped or reduced for lack of funding (2002 and 2003), or because of a major earthquake (middle of 2009). The ozone profile measurements are carried out with an Electro-Chemical Cell (ECC, 6A Science Pump Corporation®) coupled to pressure, temperature, relative humidity sensors and GPS receiver (Vaisala® RS80, RS90, RS91, and RS41-SG) with the Vaisala® MW11, DIGICORA III and MW41 sounding systems along the different periods; the flying platform is a rubber balloon (Totex® 1200 g) able to reach altitudes above 10 hPa.

In order to homogenize the data (ozone profiles), the ECC sensors preparation's procedure accurately follows the prescriptions about the sensor solution concentrations, the pump flow rate and the ECC background current measurements. The typical accuracies of pressure, temperature and relative humidity sensors are below 0.5 hPa, 0.3 K, and 2%, respectively. The ozone partial pressure profile has an overall error between 4 and 12% in the troposphere.

Temperature and pressure vertical profiles were investigated to determine the PBL stability through the calculation of temperature and potential temperature vertical gradients. The majority of historical radio-soundings made in the L'Aquila station exhibit vertical thermal stability, mainly because the safest

balloon launch procedure suggests to operate under meteorologically unperturbed conditions.

Figure 3 shows two examples of vertical temperature profiles obtained from radio sounding launches in L'Aquila: the black profile of 13 May 2015 in a night dominated by stable conditions, shows a strong thermal inversion at the ground, with dT/dz = 9.3 K hm^{-1} and $d\theta/dz$ =10 K hm^{-1}. The red vertical profile of 29 May 2014, during neutral stability conditions, presents dT/dz = − 0.5 K hm^{-1} and $d\theta/dz$ = 0.5 K hm^{-1}.

The vertical stability of the PBL is one of the fundamental parameters that can determine the accumulation of chemical substances in the lower layers of the atmosphere; it is therefore essential to check the observed near-surface radon concentration with simultaneous co-located radio-sounding profiles of pressure and temperature. Figure 4 shows the night time evolution of the radon concentration, measured on the same nights with radio-sounding temperature profiles presented as an example in Fig. 3. According to these profiles, the radon concentration during a stable night (13 May 2015; black line), grows up starting from late afternoon hours, until it reaches its maximum at the sunrise, with an accumulation of $\cong$+5.0 Bq m^{-3} h^{-1}. On the contrary, the red line shows the radon behavior during a night with neutral/unstable PBL (29 May 2014), where a null or no
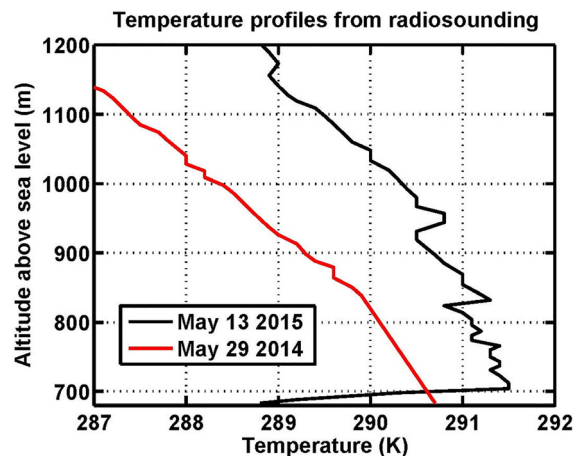

Figure 3
Vertical profiles of temperature (K) from radiosonde measurements taken in L'Aquila during 13 May 2015 (black) and 29 May 2014 (red), as examples of stable and unstable conditions (respectively) of the nocturnal PBL
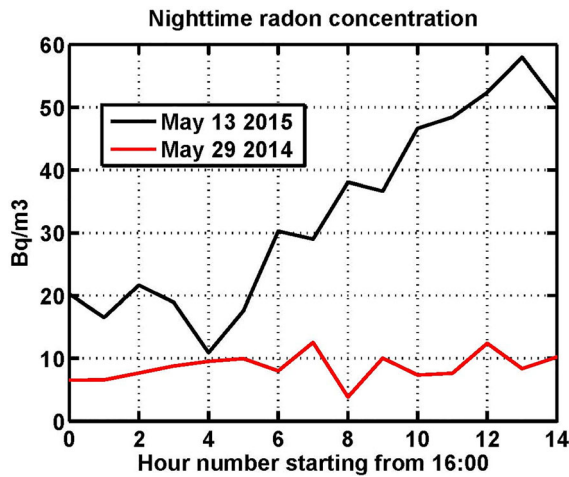
Figure 4
Night-time near-surface radon activity concentration (Bq m^{-3}) for 13 May 2015 (black) and 29 May 2014 (red), that for PBL stable and unstable conditions, respectively

significant accumulation is observed. It is evident that in case of atmospheric instability, all the radon produced at the ground is rapidly removed and diluted in the upper layers of the PBL.

2.3. Back-Trajectory Calculation

A systematic analysis of the diurnal evolution of near-surface radon concentrations, makes it clear that there are some days when the radon minimum concentration during afternoon hours is above the expected value. Once possible errors associated to the radon instrument sensitivity are excluded, the most robust physical explanation can be found in fetch effects from remote sites: these can move variable amounts of radon toward the observation site and these can superimpose to the local gas production.

The intrusion of air masses coming from the southern latitudes, presumably transiting above desert areas and potentially richer of radon, could be the cause of an unexpected radon concentration increase during daylight hours. For this reason, it was decided to analyze the path of the back-trajectories arriving in L'Aquila at 200 m a.g.l. and 500 m a.g.l. in selected days.

The chosen platform to generate back-trajectories was The Hybrid Single-Particle Lagrangian Integrated Trajectory model (HYSPLIT) developed by

NOAA's Air Resources Laboratory (Stein et al., 2015). Through the world archive site of the back and forward trajectories, it was possible to create a dataset in which the position of the air mass (latitude and longitude), pressure, air temperature and height of the PBL are reconstructed starting from 10 days before arriving in L'Aquila on the day of analysis at 1400 LT (local time = UTC + 1 h). Two different archives are chosen to run back trajectories model: the NCEP/NCAR Reanalysis with 2.5-degree latitude–longitude global grid used for 2004 events and the GDAS (Global Data Assimilation System) with 1-degree latitude–longitude grid for 2005 and 2006 events. We couldn't use the high-resolution archive for 2004 event because the data were not available for that period. Figure 5 reproduces an example of the back-trajectories reconstructed starting from the data supplied from the HYSPLIT selected archives.

3. Results and Discussion

3.1. Night-Time Radon and Surface Flux Calculation

During May 2014 and May 2015, two intensive campaigns were conducted collecting measurements of near-surface radon, ozone and meteorological parameters, as well as night time radio-sounding vertical profiles of ozone, pressure, temperature and relative humidity, on a daily basis. Two examples are presented in Fig. 4, in order to highlight the different night hour radon behaviour under opposite stability conditions of the nocturnal PBL.

The nocturnal near-surface radon changes are presented in Fig. 6 as a function of the vertical gradient of potential temperature dθ/dz, which is the classical indicator of the PBL stability and is calculated directly from the co-located radio-sounding vertical profiles of pressure and temperature. The effects of this small-scale dynamical driver are presented also in terms of the night hour near-surface ozone-changes (Online Resource 2), looking also at its pronounced anti-correlation with the radon changes (Online Resource 3 and Table 1).

The seasonal behaviour of the radon soil flux can be studied once a statistically significant number of nocturnal PBL height values are available. The
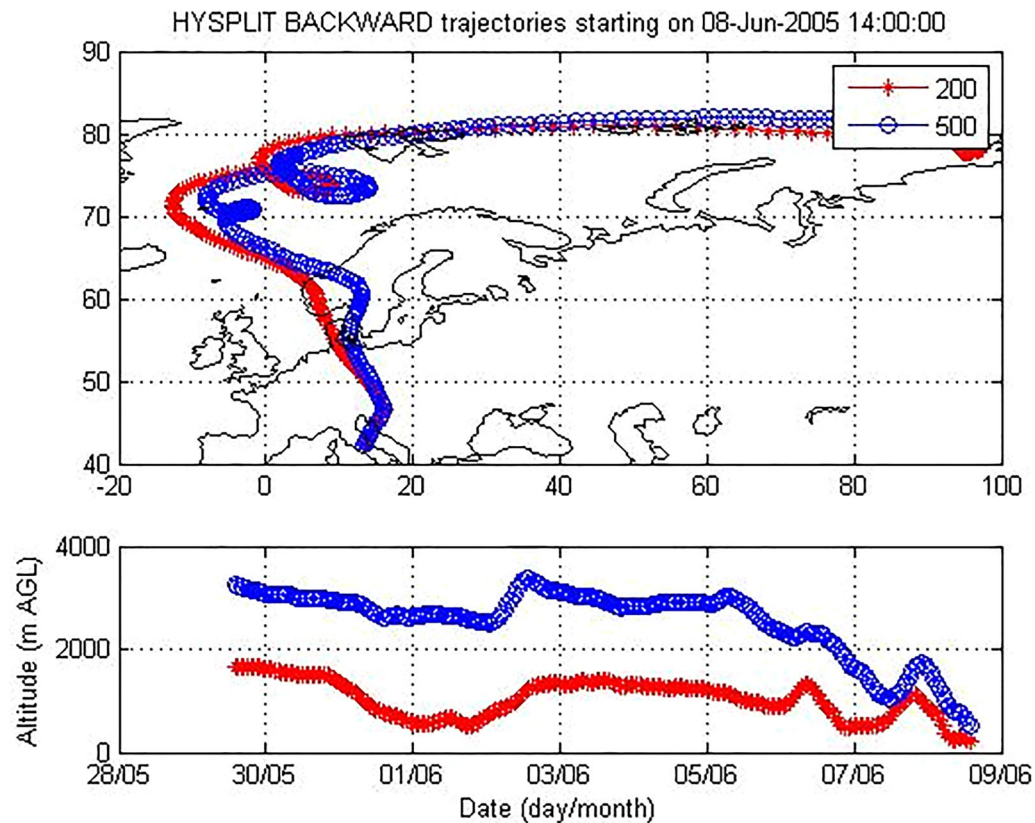
Figure 5
HYSPLIT 10-days back-trajectories for air masses arriving in L'Aquila on 8 June 2005 at 1400 LT (local time = UTC + 1 h). Panel **a** shows the latitude–longitude path for the air masses arriving in L'Aquila at 200 m altitude (red) and 500 m altitude (blue) above ground level; panel **b** shows the air mass altitude at the different lat-lon location along the path

temperature inversion altitude during meteorologically stable nights can be used as a measure of the nocturnal PBL thickness; it can be carefully measured by means of radio-sounding vertical measurements of pressure and temperature (see Fig. 3). In the absence of these profiles, it may be obtained from calculated estimates of the sensible heat flux at a single near-surface altitude level. This procedure is outlined below and was used for approximately 70% of the whole dataset reported in Fig. 7. We start from the atmospheric near-surface approximate energy balance, where the night-time tendency of potential temperature is partly controlled by the main non-adiabatic process, that is the sensible heat flux divergence between the temperature inversion top level and the surface $\alpha \, d\theta/dt = -1/(\rho c_p) \, dH/dz$. Here α is a non-dimensional scaling coefficient

(see below), θ the potential temperature (K), ρ the air density (kg m^{-3}), c_p the specific heat at constant pressure (J kg^{-1} K^{-1}), H the sensible heat flux (J m^{-2} s^{-1}).

The night-time near-surface atmosphere cools down, under meteorologically stable conditions, by providing heat for the underlying Earth surface, which in turn efficiently cools down through longwave radiative emission. The scaling coefficient α (assumed to be ≈ 0.5) is a measure of the air-cooling fraction due to sensible heat transfer to the surface, relative to the total night-time air cooling (*i.e.*, sensible heat loss plus longwave radiative cooling to space). Assuming a negligible sensible heat outflux above the layer of temperature inversion, at the finite differences we have (with $h_{inv} = \Delta z$):
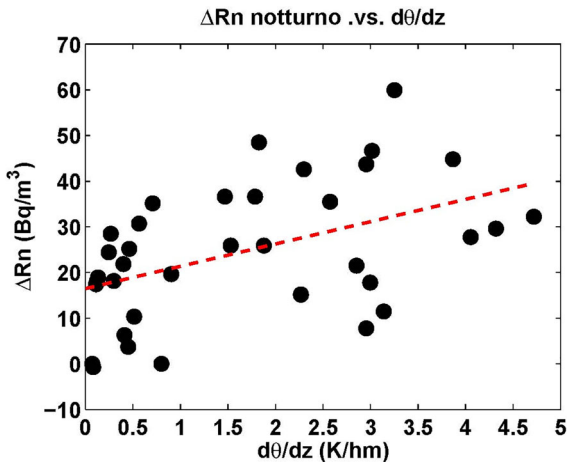
ΔRn notturno .vs. dθ/dz

Figure 6

Scatter plot of the nocturnal near-surface radon changes (Bq m^{-3}, on the y axis) (at 0600 LT with respect to 2000 LT of the previous day), versus the vertical gradient of potential temperature (θ) in the nocturnal boundary layer (K hm^{-1}, on the x axis). The temperature gradient is derived from co-located atmospheric radio-sounding measurements; data refer to days with sparse radon measurements collected during 2014–2015. A linear fit is shown with the red dashed line
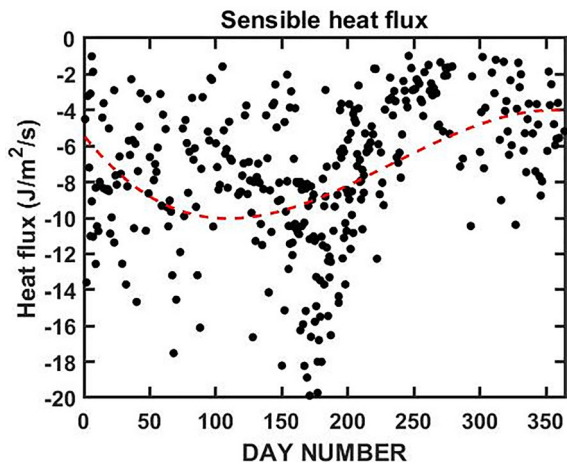
Sensible heat flux

Figure 7

Sensible heat flux (H, J m^{-2} s^{-1}), as a function of Julian day. H is calculated from Eq. (1) when radio-sounding vertical profiles of pressure and temperature are available, or following the procedure outlined in Holtslag and De Bruin, (1988) when only single-level near-surface values are available for meteorological parameters (see text and appendix). Data refer to days of years 2004–2005-2006 with a stable nocturnal PBL. A cubic fit is shown with a red dashed curve

$$H = \alpha\rho c_p \frac{\Delta\theta}{\Delta t} h_{inv}, \qquad (1)$$

$$h_{inv} = H\left(\alpha\rho c_p \frac{\Delta\theta}{\Delta t}\right)^{-1}. \qquad (2)$$

Alternatively, relating H to the vertical gradient of potential temperature ($H = -K_z \rho c_p \, d\theta/dz$) (Stull, 2012), with K_z being the vertical diffusion coefficient for a stable PBL (assumed to be ≈ 0.2 m^2 s^{-1}), we may write at the finite differences:

$$H = -K_z\rho c_p \frac{\Delta\theta}{\Delta z}, \qquad (3)$$

$$h_{inv} = -K_z \frac{\Delta\theta}{\Delta z}\left(\alpha\frac{\Delta\theta}{\Delta t}\right)^{-1}. \qquad (4)$$

Equations 2 and 4 need the knowledge of the near-surface sensible heat flux H or the vertical gradient of potential temperature dθ/dz. Both these quantities can be obtained from temperature measurements at a minimum of two altitude levels in the PBL (as clear from Eq. 3). On the other hand, however, the vertical information may not be available, as it is often the case. Some parameterizations have then been developed from which an accurate estimate of either H or dθ/dz can be obtained, using only near-surface meteorological observations. The one adopted here is described in Holtslag and De Bruin (1988) and is based on the knowledge of single-level observations of temperature, humidity and wind velocity. This method consists in the numerical solution of a near-surface energy balance equation, looking for the optimal value of the Monin–Obukhov length (which is a measure of the ratio between mechanic and buoyancy turbulence). Further details of the procedure are given in the appendix.

Once the nocturnal PBL thickness is known (in terms of the near-surface temperature inversion height) with a sufficiently robust amount of data, the seasonal behaviour of the radon soil flux can be obtained using the mass continuity equation (Li, 1974).The flux Φ is obtained assuming a negligible radon out-flux above the layer of temperature inversion and by equating the nocturnal radon time tendency (from 2000 to 0600 LT) to the surface flux divergence in the nocturnal PBL. The irreversible radon sink due to its radioactive decay is also negligible, because the e-folding time constant of approximately 5.5 days is much longer with respect

to the typical time constant of few hours for radon accumulation in the nocturnal PBL: $dRn/dt = -d\Phi/dz$. At the finite differences we have (with $h_{inv} = \Delta z$):

$$\Phi = \frac{\Delta Rn}{\Delta t} h_{inv}. \qquad (5)$$

Using Eq. 5 with the PBL thickness values of Fig. 8 and the observed nocturnal time tendency of near-surface radon (from 2000 LT of the previous until 0600 LT), we calculate the radon soil flux presented in Fig. 9, with an annually averaged value of 16 ± 6 mBq m^{-2} s^{-1} and a winter-summer positive gradient (from 12 ± 4 mBq m^{-2} s^{-1} mean value over December-January–February to 21 ± 7 mBq m^{-2} s^{-1} mean value over June-July–August), mostly explained by drier soil conditions during summer months (Pitari et al., 2015a).

The potential temperature vertical gradient (*i.e.,* the index of PBL dynamical stability) is either derived from co-located atmospheric radio-sounding measurements (when available) or obtained from the definitions of potential temperature time tendency and sensible heat flux in the nocturnal PBL (by equating Eq. 1 and Eq. 3), that is at the finite differences:

Figure 8
As in Fig. 7, but for temperature inversion height (h_{inv}, m) in the stable nocturnal boundary layer (*i.e.,* the PBL thickness measure). The temperature inversion height is obtained directly from radio-sounding vertical profiles of pressure and temperature (when available) or from Eq. 2, through the knowledge of the sensible heat flux H obtained from single-level near-surface data of meteorological parameters (see text). A cubic fit is shown with a red dashed curve

Figure 9
Surface flux of radon (mBq m^{-2} s^{-1}) obtained through Eq. 5 from the nocturnal PBL height values in Fig. 8 (see text). A cubic fit is shown with a red dashed curve

$$\frac{d\theta}{dz} = -\frac{1}{K_z} \alpha \frac{\Delta \theta}{\Delta t} h_{inv}. \qquad (6)$$

Using Eq. 6 to derive the potential temperature gradient for the whole data set presented in Fig. 8, a more robust correlation between night time changes of radon with $d\theta/dz$ can now be obtained (Fig. 10), with respect to Fig. 6, which uses only $d\theta/dz$ values from the ozone-sounding intensive campaigns of May 2014–2015. Same for the ozone ratio between the approximate time of sunrise and beginning of the
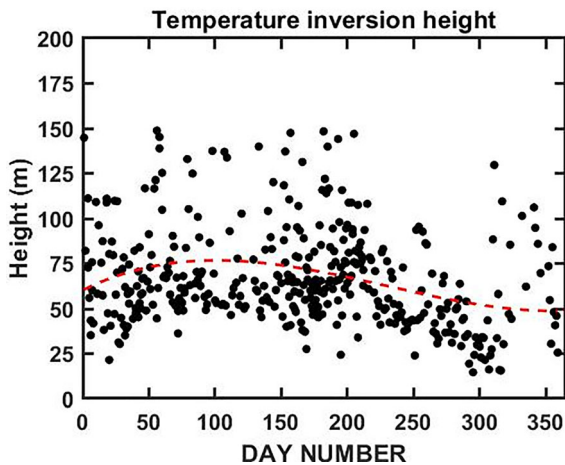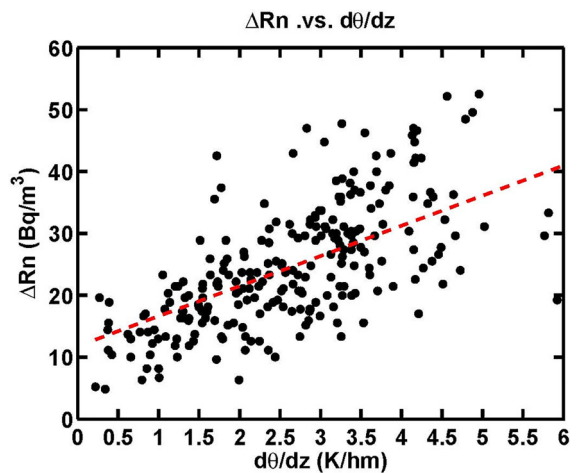

Figure 10
As in Fig. 6, but using the nocturnal radon changes of years 2004–2005-2006 for those days selected in Fig. 7. A linear fit is shown with the red dashed line

night (Online Resource 4): the efficiency of dry deposition in destroying near-surface ozone increases quasi-linearly with the PBL stability, by decreasing the ozone in-flux at the top of the temperature inversion layer.

3.2. Daytime Radon and Advection from Remote Sites

Ten-days back-trajectories from the HYSPLIT reanalysis (2004) or HYSPLIT GDAS (2005–2006) were used to trace the radon concentration in air masses arriving in the L'Aquila observational site, at 200 m and 500 m above ground level (a.g.l.). This was done for those days of years 2004–2005-2006 when continuous near-surface radon measurements were taken, regardless from the night-time PBL stability conditions and consequent level of nocturnal radon accumulation. Studying the time-dependent air mass mixing over the geographic location specified in the back-trajectory available for a given transport event, the final radon concentration over the L'Aquila site at 1400 LT was derived ($t = 0$), using back-trajectories ending at 200 m and 500 m a.g.l. The time-dependent radon concentration in the air mass moving along a given trajectory is calculated following Eq. 7, with appropriate (and simplified) assumptions for the vertical mixing:

$$Rn(t - \Delta t) = Rn(t)\exp\left(-\frac{\Delta t}{\tau_{\_dec}}\right)\exp\left(-\frac{\Delta t}{\tau_{\_mix}}\right)$$
$$+ Rn_{\_bkg}(t)\left[1 - \exp\left(-\frac{\Delta t}{\tau_{\_mix}}\right)\right], \qquad (7)$$

where:

$\Delta t = 1$ h, $\tau_{\_dec} = 5.5$ days, $\tau_{\_mix} = 3$ h [if $z(t) < h_{\_pbl}(t)$],

$\tau_{\_mix} = 30$ h [if $z(t) > h_{\_pbl}(t)$ and $z(t) < 2$ km],

$\tau_{\_mix} > \tau_{\_dec}$ [if $z(t) > 2$ km].

Δt is the time step adopted for calculating the radon changes along the trajectory, starting from $t_{in} = 240$ h; $\tau_{\_dec}$ is the radioactive decay time constant; $\tau_{\_mix}$ is the assumed small-scale convective mixing time constant; $z(t)$ is the air mass a.g.l. altitude at time t, $h_{\_pbl}(t)$ is the PBL height along the trajectory at time t; $Rn_{\_bkg}(t)$ is the steady-state background local radon concentration at time t. The numerical value of $\tau_{\_mix}$ inside the local PBL along

the trajectory (3 h) is consistent with a vertical diffusion term d/dz (K_z d$Rn_{\_bkg}$/dz), for an unstable PBL with $K_z = 20$ m^2 s^{-1}; it is also consistent with the typical dilution time of the accumulated nocturnal radon, with a typical decrease of near-surface values from 35 to 5 Bq m^{-3}, going from sunrise to noontime.

$Rn_{\_bkg}(t)$ is specified using a look-up table for the radon soil flux, built following the IAEA-WMO (2011) recommendations [$\Phi_{\_bkg}(t)$]. We start using the flux divergence for the locally produced near-surface radon. During daytime hours, following the early morning rapid dynamical dilution of the night-time accumulated radon, a quasi-steady-state radon concentration is reached. From Eq. 5 we have:

$$dRn_{\_bkg}(t) \approx 0 = -\frac{d\Phi_{\_bkg}(t)}{dz}. \qquad (8)$$

At the finite differences, d$Rn_{\_bkg}$ K_z/Δz represents the radon out-flux at the PBL top, so that, for mid-day and afternoon steady values of the radon concentration $Rn_{\_bkg}$, we may write:

$$Rn_{\_bkg}\frac{K_z}{\Delta z^2} - \frac{\Phi_{\_bkg}}{\Delta z} = 0, \qquad (9)$$

$$Rn_{\_bkg} = \Phi_{\_bkg}\frac{\Delta z}{K_z}. \qquad (10)$$

Results of $Rn(t = 0)$ are presented in Fig. 11, where $t = 0$ is the ending point of any given ten-days back-trajectory over the L'Aquila observational site. An annual average of 2.3 ± 1.3 Bq m^{-3} is calculated, with rather large day-by-day changes and a winter-summer positive gradient (from 1.6 ± 0.8 Bq m^{-3} in February to 3.0 ± 1.0 Bq m^{-3} in September). The seasonal behaviour is mostly regulated by the fraction of days in a given month with air masses originated from Northern Europe or the Atlantic Ocean, and/or spending significant amounts of time along the back-trajectory mixing with boundary layer air over the Ocean or the Mediterranean Sea. During months when this fraction is larger, the air masses arriving in the observational site have a higher probability to transport smaller amount of radon. The frequency of large-scale southerly transport events is another important regulating factor of the amount of daytime radon
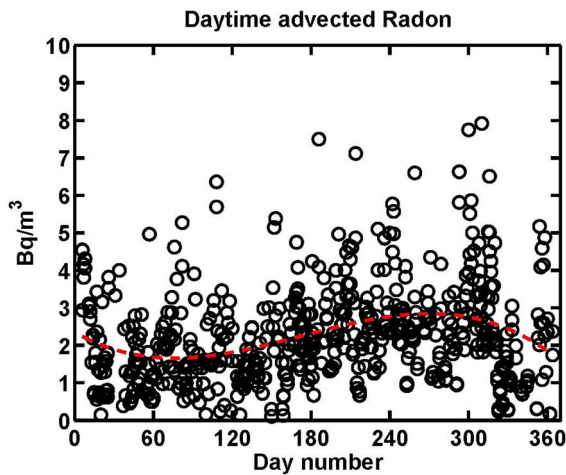
Figure 11
Calculated radon concentration (Bq m^{-3}) transported from remote sites during daytime hours, for all days of years 2004–2005-2006 when continuous near-surface radon measurements were available, regardless from the night-time PBL stability conditions and consequent level of nocturnal radon accumulation. See text for details of the horizontally transported radon calculation. A cubic fit is shown with a red dashed curve
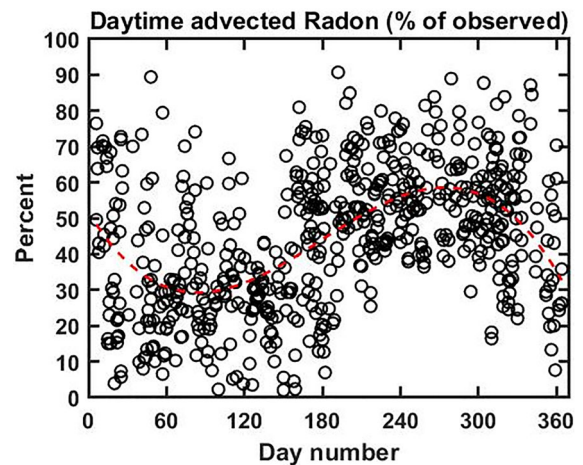

Figure 12
As in Fig. 11, but for the daytime horizontally transported radon in percent of the total observed value. A cubic fit is shown with a red dashed curve
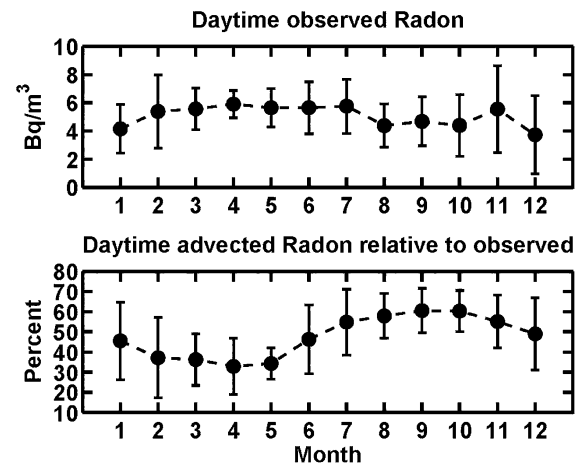

Figure 13
Monthly averages of daytime radon concentration. Observed values are shown in panel (a) (Bq m.$^{-3}$); the calculated horizontally transported radon fraction of the observed value is presented in panel (b) (percent)

imported from remote sites, due to much higher radon soil fluxes over desert surfaces (IAEA-WMO, 2011). As shown by Pitari et al. (2014), the pronounced seasonality of coarse aerosol particles observed in the L'Aquila site may be justified in a first approximation in terms of more frequent large-scale transport events from the Sahara region during late spring, summer and early autumn months, because of optimal dynamical conditions for this type of synoptic-scale southerly transport (Grams et al., 2010).

The imported radon relative weight, with respect to what is measured in the observation site during daytime hours (Fig. 12), reflects to a large extent the seasonality of transported radon discussed in Fig. 11. The calculated annual average is $44 \pm 18\%$, with a spring–autumn positive gradient (from $33 \pm 13\%$ in April to $61 \pm 10\%$ in September). In addition to this, limited impact of seasonal changes of the measured near-surface radon (Fig. 13a) has to be considered in order to properly justify the monthly mean percent amount of transported radon (Fig. 13b).

Looking at the time behaviour of monthly means (Fig. 13 and Fig. 14), one interesting feature is the large variability of the measured daytime radon during winter months. One possible reason for this,

it is that what is observed during daytime hours comes from the superposition of radon transported from remote sites (Fig. 11) and radon coming from local soil fluxes plus efficient convective mixing along the whole vertical extent of the diurnal PBL. The radon soil flux during winter months may be significantly affected in presence of snow/ice coverage or during abundant and long-lasting-large-scale precipitation events, thus increasing the day-by-day
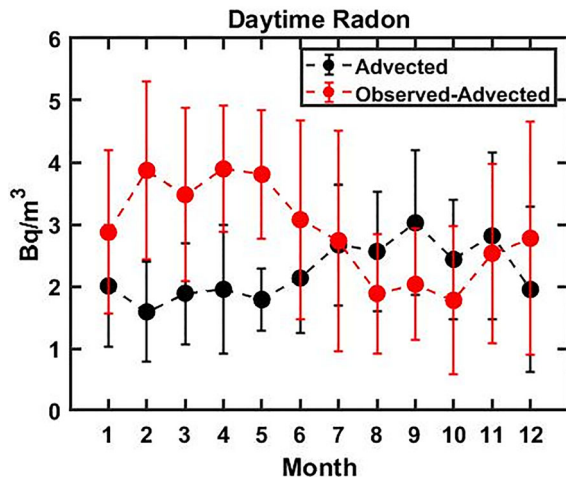
Figure 14
Monthly averages of daytime radon concentration (Bq m^{-3}). Black dots are for the calculated horizontally transported radon; red dots are for the locally produced radon, obtained as the difference between observed and transported values

radon variability and the standard deviation of wintertime monthly mean values.

An indirect check of the locally produced daytime radon can be made using the flux divergence, *i.e.,* Eq. (8–10), where now Φ represents the radon soil flux inferred from night-time measurements in the L'Aquila observation site (Fig. 9) and Rn_d is the equilibrium radon concentration during daytime hours in the site itself. In Eq. (9), $Rn_d\ K_z/\Delta z$ represents the radon out-flux at the PBL top (with $K_z \approx 5$ m^2 s^{-1} and $\Delta z \approx 1.0$ km). An estimate of Rn_d may finally be obtained through Eq. (10): $Rn_d \approx 10 \div 20$ mBq m^{-2} s^{-1} $\times$ 1000/ $5 = 2 \div 4$ Bq m^{-3}, consistent with the difference between observed and transported values in Fig. 14.

Using appropriate values of the radon flux (Fig. 9) and of the diurnal PBL height Δz (data available from the HYSPLIT reanalysis), we may compare monthly averages of the locally produced daytime radon concentration (Online Resource 5). The comparison is made between direct observations that are "cleaned up" from the calculated fetch contribution (Fig. 14) and values derived from the radon surface flux knowledge coupled to the diurnal PBL mixing (Eqs. 9–10).

The two independently calculated values of daytime radon concentration from local sources presented in the Online Resource 5 are statistically compatible, in the limits of various basic uncertainties. These uncertainties are mostly related to: (a) the fact that measured near-surface radon values during daytime hours are generally low and sometimes close to the instrument detection limit; (b) the analytical approach followed for the time-dependent radon calculation along a given back-trajectory (Eq. 7) and the confidence level of the back-trajectory itself; (c) the adopted estimates for Φ, Δz and K_z in Eq. (10).

It should be highlighted that the importance of a meaningful estimate of the long-range import of radon during daytime hours should not be seen to account for its relative contribution on monthly or seasonal means, but to properly catch the reasons for the daytime radon variability on a daily basis. Figure 12, for instance, suggests that the relative contribution of transported radon to the observed amount can be very large in many cases, reaching values up to 70–90%. This may be better highlighted looking at scatter plots of the daytime horizontally transported radon versus the near-surface observed radon values. Some examples are presented in Fig. 15: as expected from Fig. 14 we find an enhanced scatter compactness and a steeper envelope of the points during those months when the relative contribution of the transported radon is on average larger (*i.e.,* August–September-October in Fig. 15b, c, d) with respect to spring months, as March in Fig. 15a.

As previously discussed, a significant contribution to radon-rich air may come during those days with southerly transport, when back-trajectories are originated over the Sahara or (to some extent) from the Iberian Peninsula (IAEA-WMO, 2011). As a case study (April 2004), the Online Resource 6 presents two scatter plots of the daytime radon concentration versus the latitude of the air mass seven days before reaching the L'Aquila observational site at 200 m a.g.l. (Online Resource 6a) and at 500 m a.g.l. (Online Resource 6b). The important role is clear of the air mass origin latitude in regulating near-surface observed radon during daytime hours. As expected, the same behavior is featured by the calculated horizontally transported radon (Online Resource 6c).
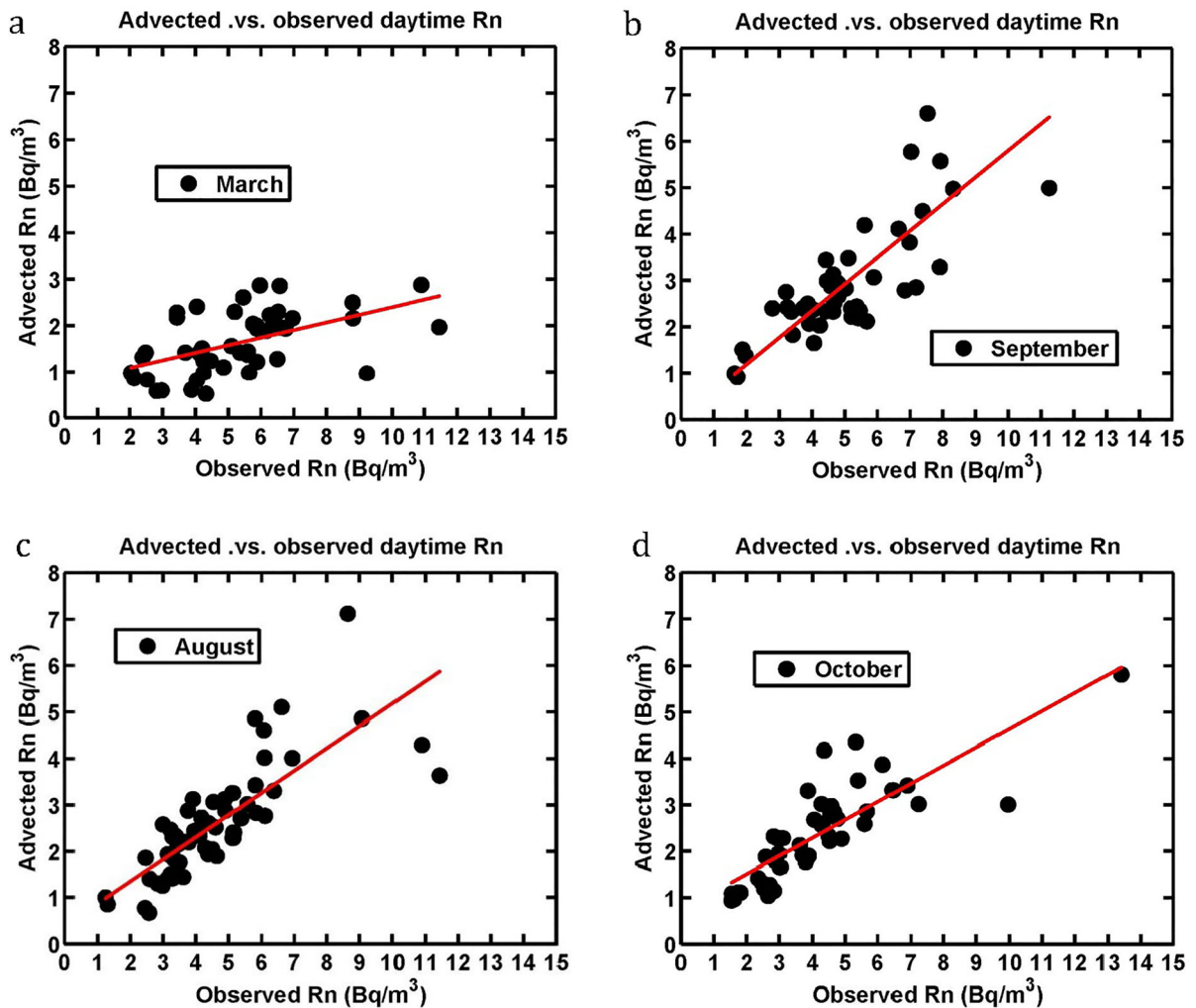
Figure 15
Scatter plots of daytime-average horizontally transported radon (Bq m^{-3}, on the y axis) and daytime-average observed radon values (Bq m^{-3}, on the x axis). Panels **a–d** refer to available days of March (**a**), August (**b**), September (**c**), October (**d**). A linear fit of the data is shown with the red lines

4. Conclusions

Radon measurements collected in a central Italy near-mountain site (L'Aquila) during years 2004–2005–2006 and 2014–2015 have been analysed to better understand the main physical mechanisms regulating the variability of atmospheric radon in the planetary boundary layer. In this work an attempt has been made to use night hour measurements of near-surface radon, ozone, meteorological parameters and pressure–temperature radio-sounding vertical profiles to infer the seasonal behaviour of the radon soil flux

in the observational site. An annual averaged flux is found in the range 16 ± 6 mBq m^{-2} s^{-1}, with a positive winter-to-summer trend. Because the instantaneous concentration of radon in the atmospheric boundary layer is controlled by a coupling of soil emission and convective mixing, stable nocturnal conditions are ideal to infer the soil emission flux from the night-time slope of the radon activity concentration.

Simultaneous measurements of meteorological parameters and ozone mixing ratios have been used as support to the radon observations, for carrying out

the above analyses and to highlight the high corre-
lation of the night hour radon accumulation with the
PBL level of stability, measured in terms of the near-
surface vertical gradient of potential temperature in
the layer of temperature inversion. The height of this
layer was carefully measured by means of radio-
sounding vertical measurements of pressure and
temperature, or in the absence of these profiles, it is
obtained from single level calculated estimates of the
sensible heat flux.

The second part of the present work was an
attempt to study the seasonal cycle and relative
weight of quasi-steady-state mid-day and afternoon
values of the near-surface radon concentration, along
with an analysis of the physical reasons behind its
variability on a daily basis. We have discussed how
nocturnal radon, on one side, is completely regulated
by local emissions coupled to more or less enhanced
stability conditions of the PBL. The much lower
radon abundance during daytime hours is, on the
other hand, only partially attributable to local sources
coupled to a vertical fast convective mixing in an
unstable diurnal PBL. Another regulating factor,
often dominant over local radon production, is the
radon import from remote sources via synoptic-scale
transport processes. Taking into account that the *e*-
folding time constant for radioactive decay of radon
is approximately 5.5 days, the effects of large-scale
transport on the observed near-surface radon during
mid-day and afternoon hours may be significant
(Chambers et al., 2011) especially with Southerly
winds. In this case, in fact, moving air masses can
bring significant amounts of radon, being originated
over the Sahara, where the radon atmospheric influx
is at least three times larger with respect to mid-lat-
itude continental sites (IAEA-WMO, 2011). With the
aid of HYSPLIT 10-days back-trajectories and a
parameterization of the PBL vertical mixing, we have
shown how day-by-day changes of daytime radon are
greatly regulated by differences in atmospheric
transport from remote sources.

Using back-trajectory reanalyses, estimates of
local radon fluxes and vertical mixing efficiencies
inside the PBL along the air mass lat-lon path and
finally the irreversible radon loss due to radioactive
decay, we have explored the fraction of daytime
radon attributable to long-range advection in the

continental near-mountain measurement site of
L'Aquila (44 $\pm$ 18%, with a spring–autumn positive
gradient, from 33 $\pm$ 13% in April to 61 $\pm$ 10% in
September). In absolute terms, we found an annual
average of daytime radon equal to
2.3 $\pm$ 1.3 Bq m^{-3}, with rather large day-by-day
changes and a winter-summer positive gradient (from
1.6 $\pm$ 0.8 Bq m^{-3} in February to 3.0 $\pm$ 1.0 Bq m^{-3}
in September). We have also highlighted how a sig-
nificant contribution to radon-rich air may come
during those days with southerly transport, when
back-trajectories are originated over the Sahara or (to
some extent) from the Iberian Peninsula.

Declarations

Conflict of Interest The authors declare no conflict of interest.

Appendix 1: Sensible Heat Estimation from Single-Level Measurements

As mentioned in Sect. 3.1, we use the simple model formulated by (Holtslag and De Bruin 1988) to estimate the sensible heat flux H in days when no vertical soundings are available, starting from weather station observations near the ground at a single height.

The method is based on the numerical solution of the surface energy balance over land:

$$H + E + G = Q \tag{11}$$

where H and E are the sensible and latent heat fluxes (positive upwards), G is the soil heat flux, and Q is the net radiation (positive downwards). Holtslag and De Bruin (1988) proposed parameterizations of the four terms as a function of the Monin–Obukhov length scale L:

$$L = \frac{u_*^2 T}{k\theta_* g}, \tag{12}$$

where u_* is the friction velocity (related to wind speed), k is the von Karman's constant ($k = 0.41$), g is the acceleration of gravity, T is the absolute temperature, and θ_* is the turbulent temperature scale, related to the sensible heat flux by:

$$H = -\rho c_p u_* \theta_*. \tag{13}$$

The input observed variables are wind speed, temperature, and relative humidity collected at weather sensor height. The algorithm consists in a numerical minimization procedure that seeks the optimal L that satisfies the equilibrium of Eq. 11, given the input variables. We use the "fzero" minimization function available in Matlab for this step. Once the optimal L is estimated for each case, the sensible heat flux H may be calculated using Eq. 13.

Publisher's Note Springer Nature remains neutral with regard to jurisdictional claims in published maps and institutional affiliations.

REFERENCES

Albert, J., Schärf, M., Enzmann, F., Waltl, M., & Sirocko, F. (2021). Local radon flux maxima in the quaternary sediments of Schleswig-Holstein (Germany). *International Journal of Earth Sciences, 110*, 1501–1516. https://doi.org/10.1007/s00531-021-02026-8

Al-Zoughool, M., & Krewski, D. (2009). Health effects of radon: A review of the literature. *International Journal of Radiation Biology, 85*, 57–69. https://doi.org/10.1080/09553000802635054

Anisimov, S. V., Galichenko, S. V., Aphinogenov, K. V., Makrushin, A. P., & Shikhova, N. M. (2017). Radon volumetric activity and ion production in the undisturbed lower atmosphere: Ground-based observations and numerical modeling. *Izvestiya, Physics of the Solid Earth, 53*, 147–161. https://doi.org/10.1134/S1069351317010037

Berezina, E. V., Elansky, N. F., Moiseenko, K. B., Belikov, I. B., Shumsky, R. A., Safronov, A. N., & Brenninkmeijer, C. A. M. (2013). Estimation of nocturnal [222]Rn soil fluxes over Russia from TROICA measurements. *Atmospheric Chemistry Physics, 13*, 11695–11708. https://doi.org/10.5194/acp-13-11695-2013

Cassiani, M., Stohl, A., & Brioude, J. (2015). Lagrangian stochastic modelling of dispersion in the convective boundary layer with skewed turbulence conditions and a vertical density gradient: formulation and implementation in the FLEXPART model. *Boundary-Layer Meteorology, 154*, 367–390. https://doi.org/10.1007/s10546-014-9976-5

Chambers, S. D., Choi, T., Park, S.-J., Williams, A. G., Hong, S.-B., Tositti, L., Griffiths, A. D., Crawford, J., & Pereira, E. (2017). Investigating local and remote terrestrial influence on air masses at contrasting antarctic sites using radon-222 and back trajectories: radon-222 at Antarctic KSG and JBS. *Journal of Geophysical Research: Atmospheres, 122*, 13525–13544. https://doi.org/10.1002/2017JD026833

Chambers, S. D., Williams, A. G., Crawford, J., & Griffiths, A. D. (2015). On the use of radon for quantifying the effects of atmospheric stability on urban emissions. *Atmospheric Chemistry*

Physics, 15, 1175–1190. https://doi.org/10.5194/acp-15-1175-2015

Chambers, S., Williams, A. G., Zahorowski, W., Griffiths, A., & Crawford, J. (2011). Separating remote fetch and local mixing influences on vertical radon measurements in the lower atmosphere. *Tellus Series B: Chemical and Physical Meteorology, 63*, 843–859. https://doi.org/10.1111/j.1600-0889.2011.00565.x

Cicerone, R. D., Ebel, J. E., & Britton, J. (2009). A systematic compilation of earthquake precursors. *Tectonophysics, 476*, 371–396. https://doi.org/10.1016/j.tecto.2009.06.008

Crawford, J., Chambers, S., Cohen, D. D., Griffiths, A., Williams, A., & Stelcer, E. (2015). Using radon-222 as an indicator of atmospheric mixing depth in ME-2 for PM2.5 source apportionment. *Aerosol Air Quality Researech, 15*, 611–624. https://doi.org/10.4209/aaqr.2014.11.0303

Di Carlo, P., Pitari, G., Mancini, E., Gentile, S., Pichelli, E., & Visconti, G. (2007). Evolution of surface ozone in central Italy based on observations and statistical model: OBSERVED AND MODELED OZONE COMPARISON. *Journal of Geophysical Research: Atmospheres.* https://doi.org/10.1029/2006JD007900

Galmarini, S. (2006). One year of 222-Rn concentration in the atmospheric surface layer. *Atmospheric Chemistry and Physics, 6*, 2865–2886. https://doi.org/10.5194/acp-6-2865-2006

Grams, C. M., Jones, S. C., Marsham, J. H., Parker, D. J., Haywood, J. M., & Heuveline, V. (2010). The Atlantic inflow to the Saharan heat low: Observations and modelling: THE ATLANTIC INFLOW TO THE SAHARAN HEAT LOW. *Quarterly Journal Royal Meteorological Society, 136*, 125–140. https://doi.org/10.1002/qj.429

Grossi, C., Vargas, A., Camacho, A., López-Coto, I., Bolívar, J. P., Xia, Y., & Conen, F. (2011). Inter-comparison of different direct and indirect methods to determine radon flux from soil. *Radiation Measurements, 46*, 112–118. https://doi.org/10.1016/j.radmeas.2010.07.021

Hirao, S., Yamazawa, H., & Moriizumi, J. (2010). Estimation of the global 222Rn flux density from the earth's surface. *Japanese Journal of Health Physics, 45*, 161–171. https://doi.org/10.5453/jhps.45.161

Holtslag, A. A. M., & De Bruin, H. A. R. (1988). Applied Modeling of the nighttime surface energy balance over land. *Journal of Applied Meteorology and Climatology, 27*, 689–704. https://doi.org/10.1175/1520-0450(1988)027%3c0689:AMOTNS%3e2.0.CO;2

IAEA-WMO, 2011. Technical meeting on sources and measurements of radon and radon progeny applied to climate and air quality studies, Proceedings of a technical meeting held in Vienna, International Atomic Energy Agency and World Meteorological Organization, ISSN 0074–1884, Vienna, Austria, 2011.

Li, T.-Y. (1974). Diurnal variations of radon and meteorological variables near the ground. *Boundary-Layer Meteorology, 7*, 185–198. https://doi.org/10.1007/BF00227912

Liu, S. C., McAfee, J. R., & Cicerone, R. J. (1984). Radon 222 and tropospheric vertical transport. *Journal of Geophysical Research, 89*, 7291. https://doi.org/10.1029/JD089iD05p07291

Perrino, C., Pietrodangelo, A., & Febo, A. (2001). An atmospheric stability index based on radon progeny measurements for the evaluation of primary urban pollution. *Atmospheric Environment, 35*, 5235–5244. https://doi.org/10.1016/S1352-2310(01)00349-1

Pitari, G., Coppari, E., De Luca, N., Di Carlo, P., & Pace, L. (2014). Aerosol measurements in the atmospheric surface layer at L'Aquila, Italy: Focus on biogenic primary particles. *Pure and Applied Geophysics, 171*, 2425–2441. https://doi.org/10.1007/s00024-014-0832-9

Pitari, G., De Luca, N., Coppari, E., Di Carlo, P., & Di Genova, G. (2015a). Seasonal variation of night-time accumulated Rn-222 in central Italy. *Environment and Earth Science, 73*, 8589–8597. https://doi.org/10.1007/s12665-015-4023-5

Pitari, G., Di Genova, G., Coppari, E., De Luca, N., Di Carlo, P., Iarlori, M., & Rizi, V. (2015b). Desert dust transported over Europe: Lidar observations and model evaluation of the radiative impact: Lidar observations of desert dust. *J. Geophys. Res. Atmospheres, 120*, 2881–2898. https://doi.org/10.1002/2014JD022875

Stein, A. F., Draxler, R. R., Rolph, G. D., Stunder, B. J. B., Cohen, M. D., & Ngan, F. (2015). NOAA's HYSPLIT atmospheric transport and dispersion modeling system. *Bulletin of the American Meteorological Society, 96*, 2059–2077. https://doi.org/10.1175/BAMS-D-14-00110.1

Stull, R. B. (2012). *An introduction to boundary layer meteorology.* Springer Science & Business Media.

Vinuesa, J.-F., Basu, S., & Galmarini, S. (2007). The diurnal evolution of < sup>222</sup>Rn and its progeny in the atmospheric boundary layer during the Wangara experiment. *Atmospheric Chem. Phys., 7*, 5003–5019. https://doi.org/10.5194/acp-7-5003-2007

Williams, A. G., Chambers, S. D., Conen, F., Reimann, S., Hill, M., Griffiths, A. D., & Crawford, J. (2016). Radon as a tracer of atmospheric influences on traffic-related air pollution in a small inland city. *Tellus Series B: Chemical and Physical Meteorology, 68*, 30967. https://doi.org/10.3402/tellusb.v68.30967

Williams, A. G., Chambers, S., & Griffiths, A. (2013). Bulk mixing and decoupling of the nocturnal stable boundary layer characterized using a ubiquitous natural tracer. *Boundary-Layer Meteorology, 149*, 381–402. https://doi.org/10.1007/s10546-013-9849-3

Zahorowski, W., Griffiths, A. D., Chambers, S. D., Williams, A. G., Law, R. M., Crawford, J., & Werczynski, S. (2013). Constraining annual and seasonal radon-222 flux density from the Southern Ocean using radon-222 concentrations in the boundary layer at Cape Grim. *Tellus Series B: Chemical and Physical Meteorology, 65*, 19622. https://doi.org/10.3402/tellusb.v65i0.19622